ELSEVIER

Biochimica et Biophysica Acta 1235 (1995) 161–168

BBA Biochimica et Biophysica Acta

Conformation, pore-forming activity, and antigenicity of synthetic peptide analogues of a spiralin putative amphipathic α helix

Catherine Brenner [a], Hervé Duclohier [b], Viktor Krchňák [c,1], Henri Wróblewski [a,*]

[a] *Département 'Membranes et Osmorégulation', CNRS URA 256, Université de Rennes 1, 35042 Rennes, France*
[b] *CNRS URA 500, Université de Rouen, 76821 Mont-Saint-Aignan, France*
[c] *Biopharm, Research Institute of Biopharmacy and Veterinary Drugs, Department of Organic Syntheses, 254 49 Jilové (near Prague), Czech Republic*

Received 8 August 1994; revised 27 December 1994; accepted 23 January 1995

Abstract

Current models depict spiralin as a bitopic transmembrane protein with the transbilayer domain being an amphipathic α helix. However, though secondary structure prediction methods suggest a helical conformation for the hypothetical transmembrane segment of spiralin, no potential transmembrane helices could be detected in this protein using the method of Von Heijne (Von Heijne, G. (1992) J. Mol. Biol. 225, 487–494). Therefore, we have reconsidered the spiralin topological model by investigating the properties of the chemically synthesized peptides SM-BC3 (LNAVNTYATLAKAVLDAIQN-NH_2) and SC-R8A2 (LNAVNTYATLASAVLEAIKN-NH_2), corresponding to the hypothetical transmembrane segments of spiralins of two distinct spiroplasma species. The hydrophobic moment plot method suggests that these spiralin amino acid stretches are class G amphipathic α helices (i.e., helices localized on the surface of a globular protein domain). Circular dichroism spectra showed that both peptides have little ordered structure in aqueous solutions but adopt a mainly helical conformation in the presence of 25% trifluoroethanol or in detergent micelles (up to 74% α helix). Both peptides formed concentration- and voltage-dependent pores in planar lipid bilayers with a unitary conductance of 130 pS in 1 M KCl and with mean numbers of monomers per conducting aggregates of 6 for SC-R8A2 and 9 for SM-BC3. However, the two peptides displayed a haemolytic activity only at high concentrations (> 250 μM) and reacted with antibodies raised against membrane-bound spiralin. Together with previously published results, these data suggest that spiralin is a monotopic membrane protein anchored at the surface of the spiroplasma cell and that the 20-residue amphipathic segment is most probably a class G helix containing a B-cell epitope.

Keywords: Alpha helix; Amphipathic helix; Antigenicity; Membrane protein; Pore-forming activity; Spiralin; Topology

1. Introduction

Owing to a small genome size (600–1700 kbp) and a cell envelope composed of only the plasma membrane, mollicutes ('mycoplasmas') are the smallest and the simplest bacteria capable of self-replication [1]. In all species analyzed so far, the membrane contains a large number of proteins modified by covalently bound fatty acids [2]. As these acylated proteins are exposed on the cell surface, they are probably involved in the interactions between mollicutes and their milieu which is in most if not all cases a human, animal, or plant host.

The plasma membrane of some species of spiroplasmas (helical-shaped mollicutes) contains a major polypeptide named spiralin which has previously been purified [3,4] and shown to being acylated, mainly by tetradecanoate (14:0) and hexadecanoate (16:0) [5]. The gene encoding spiralin has been cloned in *Escherichia coli* [6] and sequenced [7,8]. The two topological models proposed so far suggest that spiralin might be a bitopic transmembrane protein [5,8]. In the model of Chevalier et al. [8], based on secondary structure predictions from the sequence, a 20-residue amphipathic α helix lying within the last third of the polypeptide chain (Fig. 1) has been proposed as the trans-

Abbreviations: CD, circular dichroism; DOPE, dioleylphosphatidylethanolamine; Fmoc, fluorenylmethyloxycarbonyl; HPLC, high performance liquid chromatography; IgG, immunoglobulin G; POPC, palmitoyloleylphosphatidylcholine; SC-R8A2, synthetic analogue of a putative α helix of *Spiroplasma citri* strain R8A2 spiralin; SM-BC3, synthetic analogue of a putative α helix of *Spiroplasma melliferum* strain BC3 spiralin; *t*-Bu, *t*-butyl; TFE, trifluoroethanol; $\Delta\Psi$, membrane electrical potential; Δp, proton-motive force.

* Corresponding author. Fax: +33 99 286700.
[1] Present address: Selectide Corporation, 1580 East, Hanley Boulevard, Tucson, Arizona 85737, USA.

SSDI 0005-2736(95)00026-7

membrane segment of spiralin. However, evidence for the presence in prespiralin of a cleavable signal peptide [9] suggests on the other hand that spiralin is a surface anchored lipoprotein, in which case it should be devoid of any transmembrane domain. Indeed, though acylated transmembrane proteins have been found in eucaryotes [10], the overwhelming majority of all known bacterial lipoproteins are devoid of potential membrane-anchoring sequences other than the fatty acyl groups [11,12]. Due to its abundance ($\approx$ 20 to 30% membrane protein mass [3,4]), it is likely that spiralin has a structural function rather than an enzymatic one in the spiroplasma cell.

Spiralin being unrelated to any other known protein, the elucidation of its function in the spiroplasma cell requires to determine its topology and notably to decide whether or not it spans the membrane. Since the amphipathic α helix mentioned above is the strategic domain of the transmembrane model [8], we have investigated the topological propensities, the conformational properties, the pore-forming ability, the haemolytic activity, and the antigenicity of two chemically synthesized peptides, corresponding to the putative transmembrane segment of *Spiroplasma melliferum* (strain BC3) and its homologue in *Spiroplasma citri* (strain R8A2) spiralin.

2. Materials and methods

2.1. Synthesis and purification of peptides

Peptide synthesis was performed on a manually-operated multiple peptide synthesizer under continuous-flow conditions using Fmoc/*t*-Bu protection strategy as previously described [13]. Peptides were purified by preparative size-exclusion chromatography on a Sephadex G-15 2.5 × 100-cm column in 6% aqueous acetic acid (flow rate 20 ml/h) and by semi-preparative reverse-phase HPLC. The latter was carried out on 8 × 250-mm Vydac C18 columns with a flow rate of 2 ml/min and detection being monitored by UV absorption at 240 nm. Fractions containing pure peptide were pooled and lyophilized, and the purity was checked by analytical HPLC. Both peptides provided expected molecular peak in fast-atom-bombardment mass spectrometry on ZAB EQ spectrometer (VG Analytical, Manchester, UK) using Xenon gas at 8 kV and correct amino acid analysis after overnight hydrolysis at 110° C in 6 M HCl containing phenol. Furthermore, NMR analysis of the structure of the peptides confirmed that their sequences were those expected [14].

2.2. Computer-assisted sequence analysis

The topology of spiralin was investigated with the TopPred II software [15]. In this method, the strategy for predicting bacterial plasma membrane-spanning sequences is very reliable and based upon hydrophobicity analysis and charge-bias analysis (the 'positive-inside' rule) of the amino acid sequence [16,17].

Secondary structure propensities were estimated by the three following methods: CF [18,19], GOR III [20], and PHD [21]. The CF and GOR III methods are both probabilistic, using observed frequencies of amino acid residues in proteins of known structure. The CF method uses singlet frequencies and propensities whereas the GOR III method incorporates doublet frequencies derived from the protein data base. The PHD method uses multilayered (neural) networks and, according to recent evaluations, outperforms previous methods, notably when homologous sequences are available for comparison [21].

2.3. Mean hydrophobic moment calculations

Mean hydrophobic moment ($\langle \mu_H \rangle$) values of the peptides were calculated according to the method of Eisenberg et al. [22] using the following equation:

$$\langle \mu_H \rangle = \left(\left(\Sigma H_n \sin(\delta n) \right)^2 + \left(\Sigma H_n \cos(\delta n) \right)^2 \right)^{1/2} / N$$

where N is the number of residues and n is a specific residue within the peptide sequence. H_n is the hydrophobic value assigned to residue n, and δ is the angle in radians at which successive side chains emerge from the backbone when the periodic segment is viewed down its axis (e.g., 100° for the α helix). The normalized consensus hydropathy scale of Eisenberg et al. [23] and a window of 11 residues were used when $\langle \mu_H \rangle$ was plotted vs. $\langle H \rangle$. DNA Strider™ version 1.2 software [24] was used for $\langle \mu_H \rangle$ vs. δ plots.

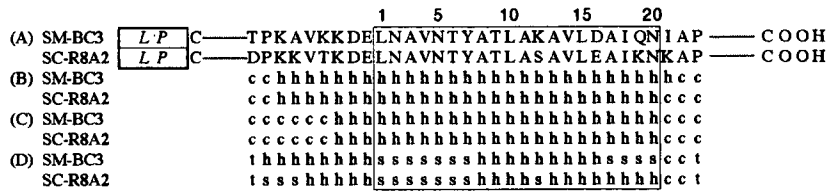

Fig. 1. Secondary structure prediction of the putative transmembrane region (framed part of the sequence) of spiralins SM-BC3 and of spiralin SC-R8A2. (A) Sequences of *S. melliferum* BC3 and of *S. citri* R8A2 spiralins [8]. LP, leader peptide [9]. Generation of secondary structure assignments: GOR III (B), PHD (C), and CF (D). Secondary structure: h, α helix; s, β sheet; t, turn; and c, coil.

2.4. Circular dichroism spectroscopy

Circular dichroism (CD) of peptide solutions was recorded from 190 to 250 nm at 20° C with a Jobin-Yvon Mark V dichrograph equipped with a thermostatically controlled quartz cell with a path length of 1 mm. The samples contained 0.3 mg of peptide per ml of 10 mM sodium phosphate buffer pH 7.2 containing or not trifluoroethanol (TFE) or detergent. Three scans were performed per analysis and subsequently averaged. Corrections were made for buffer and detergent contribution. $\Delta\epsilon$ was calculated on the basis of a mean residue mass of 115 Da and expressed in cm^{-1} M^{-1} [25].

The mean residue ellipticities at 222 nm ($[\theta]_{222}$) of these peptides were calculated by using the relationship $[\theta]_{222} = 100\ \theta/cnl$ where θ is the ellipticity (mdeg), c is the peptide concentration (mM), n is the number of amino acids in the peptide, and l is the path length (cm). The peptide α-helical content was evaluated using the following equation: $\%\ \alpha$ helix $= ((-[\theta]_{222} - 2340)/30\,300) \times 100\%$ [26]. In this equation, the values are in deg cm^2 $dmol^{-1}$.

2.5. Functional assays with planar lipid bilayers

The pore-forming activities of the two peptides were investigated at both the macroscopic and single-channel levels. The lipid mixture, POPC/DOPE (7:3, by mass) was dissolved 1% or 1‰ in n-hexane for macroscopic and patch-clamp experiments, respectively. Electrolyte on both sides of the bilayer was 1 M KCl. Peptides in stock solution were added to the *cis*- or positive side of the bilayer. For the macroscopic conductance configuration (typically, several hundred channels), virtually solvent-free bilayers were formed by the apposition of two lipid monolayers onto a 125-μm diameter hole in a 25-μm thick PTFE film sandwiched between two glass half cells [27]. For recording single-channel fluctuations, lipid bilayers were preformed at the tip of patch-clamp glass micropipettes [28] either by the droplet or the 'tip-dip' methods. Bilayer formation was monitored by the capacitance response and, prior to peptide addition, bare membranes were checked under applied potentials for electrical silence.

2.6. Assay of haemolytic activity

Human and sheep erythrocytes were prepared and haemolytic activities of the peptides were assayed as described by Bernheimer [29]. In both cases the erythrocytes were dispersed in 10 mM phosphate buffer (pH 7.4) containing 0.15 M NaCl and diluted to give a 545 nm absorbance (A_{545}) of 0.8 corresponding to 100% lysis after treatment of the cells with 2% Triton X-100. Cell suspensions were treated with different concentrations of peptides for 30 min at 37° C and A_{545} was recorded after intact cells were removed by centrifugation at 5000 rpm for 5 min at 20° C.

2.7. Dot-blot analysis

Peptide dot-blot analysis was performed as described by Canas et al. [30] using covalent attachment to Immobilon-AV membranes. Samples (5 μl containing 5, 10, or 20 μg of peptide) were applied to the membrane for 30 min to allow peptide adsorption. The primary antibodies were rabbit anti-membrane or anti-spiralin antibodies. The secondary antibodies were goat IgGs labeled with peroxidase and directed against rabbit IgGs. 4-Chloro-1-naphthol was used as the enzyme substrate [31].

3. Results

3.1. Topological propensities of S. citri and S. melliferum spiralins

Since the method of Von Heijne [17] is presently the most reliable one for the prediction of the topology of membrane proteins, notably in bacterial plasma membranes, we have used it to investigate the amino acid sequences of *S. citri* and of *S. melliferum* spiralins. In both cases, the only pointed out transmembrane segment was the N-terminal signal sequence of prespiralins. No spanning sequences were predicted in the processed form of spiralins. In transmembrane polypeptides, lysine and arginine residues (K and R, positively charged amino acid residues) are manifold more abundant than aspartic acid and glutamic acid (D and E, negatively charged amino acid residues) in cytoplasmic segments, as compared to outer segments [17]. In the model of Chevalier et al. [8], the charge-bias does not fit the 'positive-inside' rule since the ratio is 15 (K + R) and 17 (D + E) in the outer polar segment vs. 9 (K + R), and 8 (D + E) in the cytoplasmic one for *S. citri* spiralin and 22 (K + R) and 17 (D + E) in the outer polar segment vs. 6 (K + R) and 9 (D + E) in the cytoplasmic one for *S. melliferum* spiralin. However, it should be noted that it is not possible to apply this rule here as sharply as for polytopic membrane proteins, because in polar segments longer than 70 residues (which is the case for the outer polar segment of both spiralins), the content of charged residues does not seem to be dependent on their locations on either side of the membrane [32].

3.2. Secondary structure prediction and hydrophobic moment plot analysis

Fig. 1 summarizes the secondary structure predictions for the two peptides in the corresponding spiralins. For easier identification, the residues were numbered from 1 to 20 in both sequences. The GOR III method and the PHD method predict a fully α-helical conformation for both

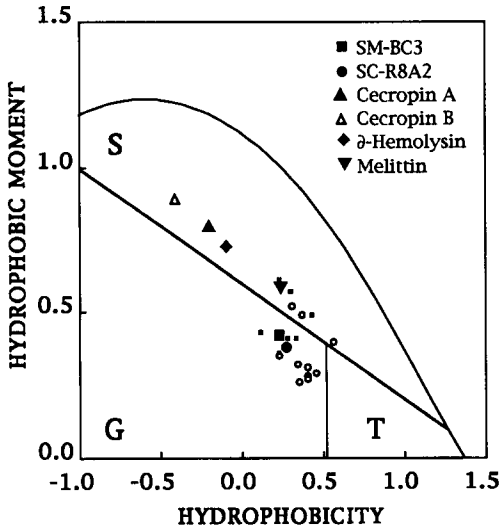

Fig. 2. Hydrophobic moment vs. hydrophobicity plots of peptides SM-BC3 and SC-R8A2. Mean hydrophobicity per residue ($\langle H \rangle$) and mean hydrophobic moment per residue ($\langle \mu_H \rangle$) were calculated using the normalyzed consensus hydrophobic scale of Eisenberg et al. [23]. Full length SM-BC3 (■) and full length SC-R8A2 (●) fall in the globular protein domain of the plot. Among the twenty 11-residue stretches scanned in the sequences of SM-BC3 (filled small square) and SC-R8A2 (○) (10 stretches for each peptide), six sequences (stretches 8–18, 9–19, and 10–20 in SM-BC3 and their homologues in SC-R8A2) fall in the surface seeking peptide domain together with cecropins A and B of *Hyalophoria cecropia*, melittin of *Apis mellifera*, and δ-hemolysin of *Staphylococcus aureus*. The fourteen other sequences fall in the same sector as full-length SM-BC3 and SC-R8A2; the coordinates of some of the points were so close that they are not resolved in the figure.

segments within their respective proteins. Both helices extend in the direction of the protein N-terminus and are interrupted on the C-terminal side by a segment of irregular structure. The helical extension predicted by the PHD method (3 residues) is shorter than that predicted by the GOR III method (6 residues). In contrast to the two previous methods, the method of Chou and Fasman (CF) predicts a shorter helical domain, localized roughly within the C-terminal side of the stretch.

The highest hydrophobic moment was observed for both peptides when $\delta = 105°$, i.e., for a α-helical structure. When the hydrophobic moment was plotted vs. the hydrophobicity, both SM-BC3 and SC-R8A2 mapped in the 'globular' protein region of the plot (Fig. 2). The twenty 11-residue sequences (10 per peptide), obtained by scanning SM-BC3 and SC-R8A2, fell in a restricted area of the Eisenberg plot. The three 11-residue sequences closest to the C-terminus of each peptide (segments 8–18, 9–19, and 10–20), i.e., those displaying the highest hydrophobic moment, laid in the 'surface' region (S) of the plot whereas all the other sequences (from 1–11 to 7–17) were found within the 'globular' region (G) of the plot. None of the peptides was found in the 'transmembrane' region (T) of the plot.

3.3. Circular dichroism (CD) spectroscopy analysis of the peptides

CD spectroscopy was used to investigate the effects of an hydrophobic environment on the conformation of SM-BC3. In a buffer containing no TFE or detergent, the peptide displayed a spectrum indicative of a mainly random coil conformation (Fig. 3), with only 18% of helical conformation detected. However, 42% of helical conformation was detected upon the addition of 10% TFE and the proportion of helices raised to 78% when the TFE concentration was increased up to 25%. The spectra ob-

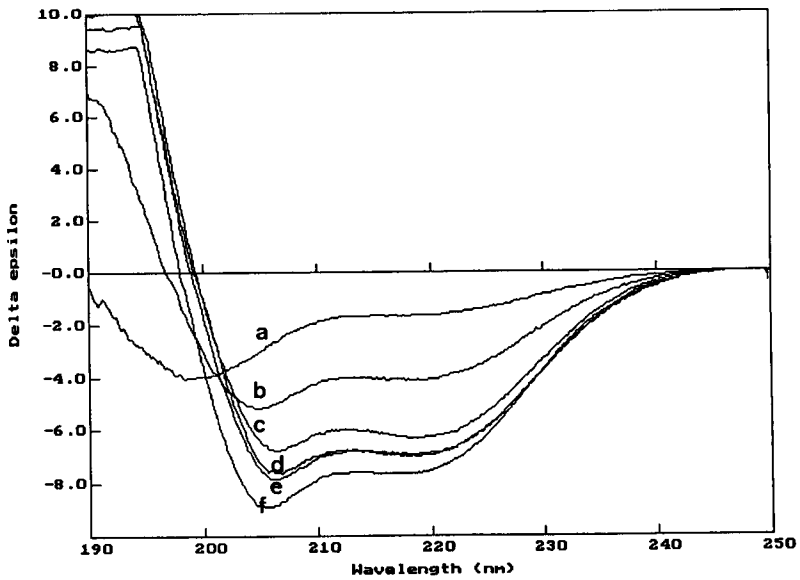

Fig. 3. Circular dichroism spectra of peptide SM-BC3 solubilized in different conditions. The polypeptide (0.3 mg/ml) was solubilized in 10 mM sodium phosphate buffer pH 7.2 (a) or in the same buffer containing 10% TFE (b), 25% TFE (f), 1% SDS (e), 1% $C_{12}E_8$ (d), or 1% octyl glucoside (c). The spectra were recorded at 20° C.

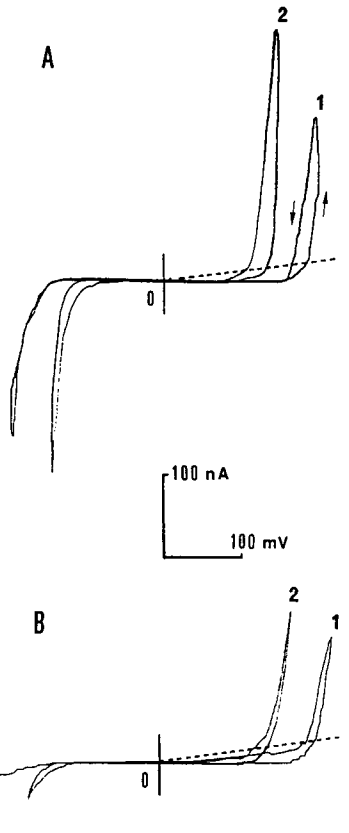

Fig. 4. Macroscopic current–voltage curves compared for peptides SM-BC3 (panel A) and SC-R8A2 (panel B) in POPC/DOPE planar bilayers, at two aqueous concentrations, curves 1: $2 \cdot 10^{-6}$ M and curves 2: $4 \cdot 10^{-6}$ M (*cis*-side). Electrolyte: 1 M KCl both sides; room temperature. Characteristic voltages are defined by the crossings of the exponential branches (raising limb) with a reference conductance (broken line, 150 nS). ∅= 125 μm.

tained when the peptide was solubilized in the presence of different detergents were similar to those recorded in the presence of 25% TFE. Specifically, the proportions of helices were 74, 73, and 65% for SM-BC3 solubilized in the presence of 1% SDS, 1% $C_{12}E_8$, or 1% octyl glucoside, respectively. The conformation of SC-R8A2 was analyzed in buffer devoid of TFE or detergent, in the presence of 25% TFE, and in the presence of 1% octyl glucoside. The spectra (data not shown) were not significantly different from those recorded with SC-R8A2.

3.4. Ion conductances induced by peptides SM-BC3 and SC-R8A2 in planar lipid bilayers

In the macroscopic conductance configuration, adding $2 \cdot 10^{-6}$ M peptide to the *cis*-side of the bilayer (an estimation of the intrinsic peptide concentration within the bilayer will be given in Discussion) led, within 10 to 15 min, to the development of highly voltage-dependent currents both for positive and negative voltages (Fig. 4). After equilibrium was reached, V_c, the characteristic voltage at which the exponential branch crossed a reference conductance was noted and the peptide bath concentration doubled. Results for both analogues are summarized and analyzed in Table 1. From concentration- and voltage-dependencies, an analysis previously described for alamethicin, the prototype of pore-forming peptides through the aggregation of amphipathic helical monomers [33], allows to derive N, the apparent and mean number of monomers per conducting aggregate. $N = V_a/V_e$, where V_a is the characteristic voltage shift for an e-fold change in concentration and V_e the voltage increment resulting in an e-fold change in conductance. Note the quasi-symmetry in these (I–V) current–voltage curves, higher thresholds (V_c) for SC-R8A2 peptide but a significantly reduced voltage-dependence as compared to SM-BC3. The size of the aggregates appear higher too, with the latter analogue.

With slightly reduced aqueous peptide concentrations and bilayers at the tip of patch-clamp micropipettes (internal diameter around 1 μm), single-channel current fluctuations were recorded. For example in the case of SM-BC3, within long bursts of activity, unitary current rapidly flickered between hardly resolved closed and open states (not shown). The unit conductance was 130 pS in 1 M KCl and the probability for the open state was about 0.8 at 150 mV.

3.5. Haemolytic activity of peptides SM-BC3 and SC-R8A2

Fig. 5 shows the haemolysis of human and sheep erythrocytes as a function of the concentration of SM-BC3 and of SM-R8A2. There was no lytic activity for SC-R8A2 for concentrations ≤ 100 μM. Beyond that concentration threshold, 44% of human erythrocytes and 25% of sheep erythrocytes were lysed with 250 μM SC-R8A2. At high

Table 1
Analysis of conductance data

Peptides	Concentration-dependence			Voltage-dependence	N
	V_{c1} (mV)	V_{c2} (mV)	V_a (mV)	V_e (mV)	
SM-BC3	170	117	71	7.6	9
SC-R8A2	204	148	75	12.5	6

V_{ci}, characteristic voltage at which the ascending limb of the exponential branch of current crosses a reference conductance. Peptide concentrations: $2 \cdot 10^{-6}$ M and $4 \cdot 10^{-6}$ M for V_{c1} and V_{c2}, respectively. $V_a = 0.5\Delta V_c \times e$, with e = 2.78. N, mean number of monomers per conducting aggregate [32].

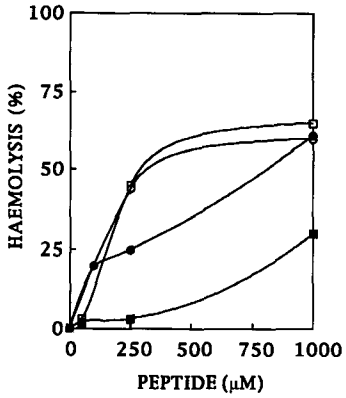

Fig. 5. Erythrocyte lysis by peptides SM-BC3 and SC-R8A2. Human or sheep erythrocyte suspensions were exposed to varying concentrations of peptide SM-BC3 or of peptide SC-R8A2 and the amount of released hemoglobin was determined by measuring the absorbance at 545 nm (A_{545}). Complete lysis (100%) was obtained by the addition of 2% Triton X-100 to the cell suspensions. Symbols: activity of SM-BC3 on human erythrocytes (□) and on sheep erythrocytes (■); activity of SC-R8A2 on human erythrocytes (○) and on sheep erythrocytes (●).

concentration (1 mM peptide), 60% of erythrocytes were lysed in both cases. The haemolytic activity of SM-BC3 was similar to that of SM-R8A2 in the case of human erythrocytes but significantly weaker in the case of sheep erythrocytes with 3% of lysis at a concentration of 250 μM and 30% at 1 mM. In the assay, no spontaneous haemolysis was observed in the absence of peptide. In comparison, melittin induced 100% lysis in human erythrocytes and in sheep erythrocytes at concentrations ≥ 0.03 μM and ≥ 3.5 μM, respectively.

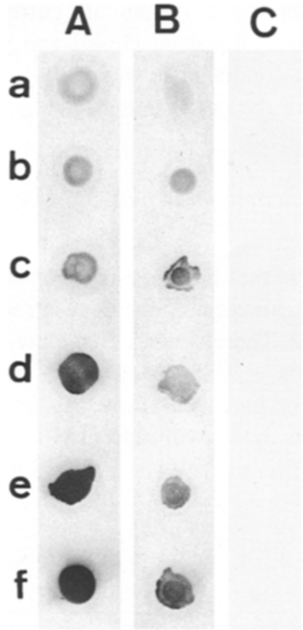

Fig. 6. Dot-blot immunodetection of peptides SM-BC3 and SC-R8A2. Antigens: SM-BC3 (a, b, and c: 5, 10, and 20 μg of peptide, respectively) and SC-R8A2 (d, e, and f: 5, 10, and 20 μg of peptide, respectively). Antibodies: anti-spiralin SC-R8A2 (A and D), anti-spiralin SM-BC3 (B and E), and anti-membrane of *M. gallisepticum* (C and F). The sera were used at a 50-fold dilution.

3.6. Antigenicity of peptides SM-BC3 and SC-R8A2

Since B-cell epitopes are specific targets of the binding sites of B-cell immunoglobulin receptors and circulating antibodies, antibodies elicited by a protein in its native conformation are specific for surface determinants of the intact three-dimensional structure of the protein. To assess whether peptides SM-BC3 and SC-R8A2 are B-cell epitopes we have tested their reactivity with antibodies elicited with native, membrane-bound spiralin.

The dot-blot analysis revealed that peptides SM-BC3 and SC-R8A2 covalently attached to Immobilon-AV membranes were capable of binding antibodies raised against native spiralin (Fig. 6). In contrast, antibodies raised against membrane proteins of *Mycoplasma gallisepticum* (a species which, as spiroplasmas, also belongs to the *Mollicutes* class of eubacteria) were not bound by the peptides (C and F in Fig. 6). In these experiments, the homologous antigen-antibody reaction between peptide SC-R8A2 and anti-*S. citri*-R8A2 spiralin antibodies gave, as expected, a stronger label than the heterologous reaction between peptide SM-BC3 and anti-*S. citri*-R8A2 spiralin antibodies (compare A and D in Fig. 6). However, the reverse was not true since antibodies directed against *S. melliferum*-BC3 spiralin gave a stronger label in the heterologous reaction (compare B and E in Fig. 6). The results of the dot-blot analysis indicate that the two synthetic peptides contain a B-cell epitope identical or similar to an antigenic determinant localized on the surface of spiralin.

4. Discussion

Two of the three algorithms used in this study to predict secondary structure (PHD and GOR III methods vs. CF method) suggested a fully helical conformation for the two homologous 20-residue segments of spiralin of *S. citri* R8A2 and *S.* melliferum BC3. This was experimentally confirmed by analyzing the solution conformation of two synthetic analogs of these sequences. Circular dichroism (CD) spectra of the peptides solubilized into different media revealed that peptide helicity was significantly enhanced only in the presence of TFE as a co-solvent or in the presence of surfactant micelles. Since the use of high concentrations of TFE in conformation studies may be misleading, it should be stressed that in the present study, peptide CD spectra were recorded at low TFE concentrations (≤ 25%). It should also be noted that the helical conformation of SM-BC3 in 30% TFE was demonstrated by NMR spectroscopy [14]. It was furthermore shown in this latter analysis that the sequence encompassing residues 4 to 20 (see Fig. 1) formed an amphipathic α helix

whereas the three N-terminal residues (L-N-A) displayed a much more flexible conformation.

Three main types of helices can be discriminated by the hydrophobic moment plot: membrane spanning helices (class T helices), membrane surface seeking helices (class S helices), and globular protein helices (class G helices) [22,23]. The two peptides SM-BC3 and SC-R8A2 were identified by this method as class G helices with, however, characteristics making them not too different from class S helices. This was experimentally confirmed by two facts. Firstly, both peptides were capable of forming voltage-dependent pores as do membrane seeking α-helical amphipathic polypeptides such as alamethicin [33,34] or amphipathic α-helical transmembrane segments of channel proteins [35,36]. We thus assume that the pores formed by SM-BC3 and SC-R8A2 result from helices clustering under the form of a bundle perpendicular to the plane of the membrane with hydrophilic sidechains lining the central, ion-conducting pore and hydrophobic sidechains interacting with the fatty acyl chains of the lipids (for review see [37–39]). Secondly, these peptides displayed a haemolytic activity as expected from surface seeking polypeptides. However, haemolytic activity toward both human and sheep erythrocytes was significant at only very high concentrations. Indeed, 0.25 to 1 mM peptide concentrations were required to achieve about 50% haemolysis whereas, in the same conditions, 100% lysis was observed with about 1 μM melittin (Fig. 5). Since the haemolytic activity of amphipathic peptides is highly dependent on their content in positively charged amino acid residues [40], the low haemolytic activities of SM-BC3 and SC-R8A2 are probably due to the fact they contain only two charged amino acids: one basic residue (K in both cases) and one acidic residue (D in SM-BC3 and E in SC-R8A2).

A comparison of these concentrations with those needed in the bulk to induce a pore-forming activity in planar lipid bilayers is not straightforward. The actual or intrinsic peptide concentration in the bilayer can only be tentatively estimated. The ratio of macroscopic conductance at a given voltage and concentration to the average-single channel conductance (amplitude $\times$ probability of opening) represents the number of *available* conducting aggregates in the bilayer, e.g., $2 \cdot 10^4$ for SM-BC3 at 150 mV and $4 \cdot 10^{-6}$ M. Thus, the conducting aggregate density is $1.7 \cdot 10^8$ per cm^2 or since $N = 9$ (monomers per conducting aggregate), the overall density of peptide monomers involved in the pore forming activity would be about $1.5 \cdot 10^9$ per cm^2 of planar lipid bilayer. Assuming 70 $Å^2$ for the average cross-sectional area of a phospholipid molecule, we arrive at an apparent peptide (involved or available in pore formation)/lipid of 10^{-5}. Ultimately, this figure would have to be compared with the whole protein (spiralin) density in situ whence new models for its topology will be devised. Finally, it is worth noting that the number of monomers involved in pore-forming activity is only a minor fraction of the total number of monomers in or associated with the bilayer, according to a recent study with alamethicin [41].

With regard to macroscopic conductance data, lower V_c thresholds (Fig. 5), higher voltage-dependence (Fig. 5), and larger number of helices per bundle (Table 1) for SM-BC3 as compared to SC-R8A2 are probably due to the position of the lysyl residue along the sequence (Fig. 1). Indeed, the major difference between the two peptides lies in the position of the lysyl residue which is close to the middle of SM-BC3 and thus more likely to feel the transmembrane field, whereas in SC-R8A2 this charged residue is situated just before the C-terminus.

These data thus provide a theoretical and experimental support for an amphipathic α-helical conformation of the homologous stretches comprising residues 139 to 168 in spiralin of *S. citri* R8A2 and residues 143 to 162 in spiralin of *S. melliferum* (numbering of the residues is as in [7,8] minus the 23-residue signal sequence [9]). However, they suggest that, in contrast to the model depicting spiralin as a bitopic membrane protein [5,8], these segments do not span the spiroplasma membrane. It should also be noted that owing to the very high abundance of spiralin in the spiroplasma cell (about 25% of the membrane intrinsic protein fraction [3,4]), the presence of such channels in the plasma membrane might be lethal to the bacterium if a threshold potential is reached. Indeed, the concentration dependence shown in Fig. 4 suggests that the transmembrane potential of spiroplasmas ($\Delta\Psi = -80$ mV and $\Delta p = -123$ mM [42]) might be large enough to enhance the pore-forming activity of the peptides, especially if the latter are present at high concentration in the membrane which is the case of spiralin [3,4].

Though the hypothesis of a membrane surface helix cannot yet be definitively ruled out, other lines of argument strongly suggest that the α helix evidenced in spiralin is localized at the surface of a globular domain of the protein. This interpretation is supported by the fact that this helix contains a B-cell epitope capable of binding antibodies raised by native, membrane-bound spiralin. Incidently, the cross-reactions between the two peptides suggest that this epitope is probably involved in the antigenic relatedness observed between the spiralins of *S. citri* and *S. melliferum* [43]. The obtention of antibodies raised specifically against this epitope will hopefully allow to determine its precise localization in the protein and its accessibility to antibodies on the spiroplasma cell surface.

Spiralin containing a cleavable N-terminal signal sequence [9] and being acylated [5] is probably a monotopic protein bound onto the outer leaflet of the plasma membrane of spiroplasmas by its lipidic moiety, which seems to be a rule amongst bacterial plasma membrane-bound acyl proteins [11,12]. This monotopic model of spiralin is furthermore corroborated with the absence of any transmembrane segment, as predicted by the method of Von Heijne [17] in the processed form of *S. citri* and *S. melliferum* spiralins.

Acknowledgements

We thank Emmanuel Shechter for useful advices regarding CD spectroscopy and Noëlle Genetet for the generous gift of human and sheep erythrocytes. This work was supported by the Groupement de Recherches 'Peptides et Protéines Amphiphiles' (GDR 1153, CNRS), the Groupement de Recherches 'Systèmes Colloïdaux Mixtes' (GDR 1082, CNRS and CEA), the Langlois Foundation (Rennes), and the Région Bretagne (Programme BRITTA).

References

[1] Razin, S. (1992) FEMS Microbiol. Lett. 100, 423–432.
[2] Wieslander, Å., Boyer, M. and Wróblewski, H. (1992) in Mycoplasmas: Molecular Biology and Pathogenesis (Maniloff, J., McElhaney, R.N., Finch, L.R. and Baseman, J.B., eds.), pp. 93–112, American Society for Microbiology Publications, Washington, DC.
[3] Wróblewski, H., Johansson, K.-E. and Hjertén, S. (1977) Biochim. Biophys. Acta 465, 275–289.
[4] Wróblewski, H., Robic, D., Thomas, D. and Blanchard, A. (1984) Ann. Inst. Pasteur Microbiol. 135A, 73–82.
[5] Wróblewski, H., Nyström, S., Blanchard, A. and Wieslander, Å. (1989) J. Bacteriol. 171, 5039–5047.
[6] Mouchès, C., Candresse, T., Barroso, G., Saillard, C., Wróblewski, H. and Bové, J.M. (1985) J. Bacteriol. 164, 1094–1099.
[7] Chevalier, C., Saillard, C. and Bové, J.M. (1990) J. Bacteriol. 172, 2693–2703.
[8] Chevalier, C., Saillard, C. and Bové, J.M. (1990) J. Bacteriol. 172, 6090–6097.
[9] Le Hénaff, M., Brenner, C., Fontenelle, C., Delamarche, C. and Wróblewski, H. (1991) C.R. Acad. Sci. Paris, Sér. III 312, 189–195.
[10] Towler, D.A., Gordon, J.I., Adams, S.P. and Glaser, L. (1988) Annu. Rev. Biochem. 57, 69–99.
[11] Hayashi, S. and Wu, H.C. (1990) J. Bioeng. Biomembr. 22, 451–471.
[12] Pugsley, A.P. (1993) Microbiol. Rev. 57, 50–108.
[13] Krchňák, V. and Vágner, J. (1990) Pept. Res. 3, 182–193.
[14] Bondon, A., Berthault, P., Segalas, I., Perly, B. and Wróblewski, H. (1995) Biochim. Biophys. Acta 1235, 169–177.
[15] Claros, M.G. and Von Heijne, G. (1995) Comp. Appl. Biosci. 10, 685–686.
[16] Von Heijne, G. (1986) EMBO J. 5, 3021–3027.
[17] Von Heijne, G. (1992) J. Mol. Biol. 225, 487–494.
[18] Chou, P.Y. and Fasman, G.D. (1974) Biochemistry 13, 222–245.
[19] Chou, P.Y. and Fasman, G.D. (1978) Adv. Enzymol. 47, 45–148.
[20] Gilbrat, J.-F., Garnier, J. and Robson, B. (1987) J. Mol. Biol. 198, 425–443.
[21] Rost, B. and Sander, C. (1993) J. Mol. Biol. 232, 584–599.
[22] Eisenberg, D., Weiss, R.M. and Terwilliger, T.C. (1982) Nature 299, 371–374.
[23] Eisenberg, D., Schwarz, E., Komaromy, M. and Wall, R. (1984) J. Mol. Biol. 179, 125–142.
[24] Marck, C. (1988) Nucleic Acids Res. 16, 1829–1836.
[25] Yang, J.T., Wu, C.-S.C. and Martinez, H.M. (1986) Methods Enzymol. 130, 208–269.
[26] Chen, Y.-H., Yang, J.T. and Martinez, H.M. (1972) Biochemistry 11, 4120–4131.
[27] Montal, P. and Mueller, P. (1972) Proc. Natl. Acad. Sci. USA 69, 3561–3566.
[28] Hanke, W., Methfessel, C., Wilmsen, U. and Boheim, G. (1984) Bioelectrochem. Bioenerg. 12, 329–339.
[29] Bernheimer, A.W. (1988) Methods Enzymol. 165, 213–217.
[30] Canas, B., Dai, Z., Lackland, H., Poretz, R. and Stein, S. (1993) Anal. Biochem. 211, 179–182.
[31] Hawkes, R., Niday, E. and Gordon, J. (1982) Anal. Biochem. 119, 142–147.
[32] Von Heijne, G. and Gavel, Y. (1988) Eur. J. Biochem. 174, 671–678.
[33] Hall, J.E., Vodyanoy, I., Balasubramamian, T.M. and Marshall, G.R. (1984) Biophys. J. 45, 233–247.
[34] Boheim, G. (1974) J. Membr. Biol. 19, 277–303.
[35] Oiki, S., Madison, V. and Montal, M. (1990) Proteins 8, 226–236.
[36] Brullemans, M., Helluin, O., Dugast, J.-Y., Molle, G. and Duclohier, H. (1994) Eur. Biophys. J. 23, 39–49.
[37] Cafiso, D.S. (1994) Annu. Rev. Biophys. Biomol. Struct. 23, 141–165.
[38] Sansom, M.S.P. (1991) Progr. Biophys. Mol. Biol. 55, 139–235.
[39] Spach, G., Duclohier, H., Molle, G. and Valleton, J.M. (1989) Biochimie 71, 11–21.
[40] Cornut, I., Thiaudière, E., and Dufourcq, J. (1993) in The Amphipathic Helix (Epand, R.M., ed.), pp. 173–219, CRC Press, Boca Raton, FL.
[41] Archer, S.J., Ellena, J.F. and Cafiso, D.S. (1991) Biophys. J. 60, 389–398.
[42] Schummer, U. and Schiefer, H.G. (1987) FEBS Lett. 224, 79–82.
[43] Zaaria, A., Fontenelle, C., Le Hénaff, M. and Wróblewski, H. (1990) J. Bacteriol. 172, 5494–5496.